

INVESTIGATION OF THE 3D DISPLACEMENT CHARACTERISTICS FOR A MACRO-FIBER COMPOSITE TRANSDUCER (MFC-P1)

RAZISKAVA 3D KARAKTERISTIK ODMIKA PRETVORNIKA IZ KOMPOZITA Z MAKROVLAKNI (MFC-P1)

Kumar Anubhav Tiwari, Renaldas Raisutis

¹Ultrasound Institute, Kaunas University of Technology, K. Barsausko St. 59-A420 51423 Kaunas, Lithuania
k.tiwari@ktu.lt

Prejem rokopisa – received: 2017-10-04; sprejem za objavo – accepted for publication: 2017-10-26

doi:10.17222/mit.2017.166

The accurate three-dimensional (3D) displacement profile of a contact-type ultrasonic transducer ensures that the transducer is free of defects during its manufacturing or installation. It also ensures the applicability of the transducer in structural health monitoring (SHM) and non-destructive testing (NDT). Since its invention in 1996 by NASA, the macro-fiber composite (MFC) transducer was positively accepted by researchers due to its lightweight, flexibility, durability and reliability. As it can be embedded quite easily on the structure under inspection, there are different ways to which it can be used for the detection of defects in the composite materials using guided Lamb waves. The objective of the presented work was to investigate the operational performance of an unloaded macro fiber composite (MFC) transducer of P1-type by estimating its 3D displacement components. The 3D spatial displacements of vibrating MFC were investigated using a Polytec 3D scanning laser vibrometer (PSV-500-3D-HV) in order to determine the directions/planes along which the ultrasonic guide waves would be generated most effectively. The behaviour of the MFC transducer of P1 type based on the displacement characteristics confirmed that it works in d33 (elongation) mode, as specified in the manufacturer's specifications.

Keywords: macro fiber composite, ultrasonic NDT, spatial displacements, Lamb waves, 3D-scanning laser vibrometer

Natančen tridimenzionalni profil (3D) premikov kontaknega ultrazvočnega pretvornika omogoča, da je le-ta brez napak med izdelavo ali namestitvijo. To namreč zagotavlja uporabnost pretvornika za strukturno zdravstveno opazovanje (angl. SHM) in neporušno testiranje materialov (angl. NDT). NASA je leta 1996 izumila ultrazvočni kompozitni pretvornik na osnovi makrovlaknen (MFC; angl.: Macro-Fiber Composite). Raziskovalci so potem pretvornik kmalu pozitivno sprejeli zaradi njegove majhne mase, prilagodljivosti, trajnosti in zanesljivosti. Obstajajo različni načini njegove uporabe za odkrivanje napak v kompozitnih materialih z uporabo kontroliranih Lambovih valov, ker ga je zelo lahko namestiti na preiskovano strukturo. Predmet raziskave predstavljene v tem članku, so lastnosti obratovanja neobremenjenega MFC-pretvornika tipa P1 z oceno njegovih 3D-premikov. Prostorske premike vibrirajočega MFC so avtorji preiskovali s 3D-laserskim skenirnim vibrometrom Polytec (PSV-500-3D-HV) in s tem določili smeri in ravnine, vzdolž katerih so vodeni ultrazvočni valovi najbolj učinkovito generirani. Potrdili so, da le-ta deluje v načinu d33 (raztezek) in da so karakteristike obnašanja MFC pretvornika tipa P1 v skladu s proizvajalčevo specifikacijo.

Ključne besede: kompozit iz makrovlaknen, ultrazvočna neporušna preiskava (NDT), prostorski premiki, Lambovi valovi, 3D-laserski skenirni vibrometer

1 INTRODUCTION

The compact size and low weight, flat geometrical profile, ability to work as an actuator in the transmission mode as well as a sensor in the reception mode makes the macro fiber composite (MFC) the best available choice for non-destructive testing (NDT) and structure health monitoring (SHM) of the structures.¹⁻⁴ One of the best features of the MFC transducer is that MFC is an efficient transmitter/receiver for generating/receiving the A0 and S0 modes of guided Lamb waves.⁵⁻⁶ Hence, it can be easily combined with the available contact and non-contact ultrasonic techniques for the inspection of structures.⁷ Embedded MFCs are widely used in aerospace for generating ultrasound waves, harvesting energy, and also for the detection of defects due to impact.⁸ The aerodynamic performance of flexible wings and the overall efficiency of the structure can be effec-

tively improved by the ability of MFCs to control the aerodynamic shaping of the airfoils and the twisting motion of the wings.⁹⁻¹⁰ The fiber volume fraction of MFC is 0.824, which is more than AFC. This is also one of the reasons for having the high performance and stiffness of the MFC. The actuation performance of the MFC is not only better than the AFC (1.5 times), but also better than most widely used piezoceramic actuators.⁹⁻¹⁰ The general characteristics and features of MFC-2814-P1 are briefly shown in **Table 1**.

The displacement characteristics are an effective way of analysing transducer behaviour and spatial displacements. Any perturbation in the displacement characteristics would lead to generating non-standard beams of in-plane and out-of-plane components during the generation of ultrasonic guided waves (GW).¹¹ Hence, the defected transducers can be omitted from the

experimental analysis or applications in SHM tasks. The prior estimation of the displacement characteristics of the transducer is also applicable in the design of a transducer array or to manufacture the new transducers with specific characteristics. By knowing the spatial displacement of the transducer, the analytical modelling of the transducers can also be improved.¹²

Table 1: General characteristics of MFC-P1-M2814 (from Smart Material Corporation)

Features	Typical value
Active (length × width)	28 mm × 14 mm
Overall (length × width)	38 mm × 20 mm
Capacitance	1.15 nF
Free strain	0.155 %
Blocking force	195 N
Operating voltage	-500 V to +1500 V
Operating bandwidth as a sensor	0 Hz to 1 MHz
Operating bandwidth as an actuator	0 Hz to 700 kHz
Maximum operational tensile strain	< 0.45 %
Linear-elastic tensile strain limit	0.1 %

The objective of the presented work was to investigate the spatial displacement characteristics of the MFC transducer and its applicability in ultrasonic NDT and SHM by guided waves. First, the impedance and phase characteristics of the unloaded MFC-P1 type transducer were measured using the impedance meter in order to find the resonant frequency of the transducer. Later, the 3D spatial displacements were measured using a 3D scanning laser vibrometer.

2 EXPERIMENTAL PART

For the experimental analysis, MFC-P1-2814 (S.n. 08J100791) manufactured by *Smart Materials*¹ was investigated. The entire experimental process was conducted in two steps. In the first step, the impedance and phase characteristics of the MFC were measured using an impedance analyzer (Wayne Kerr 6500B). The schematic diagram and frequency-dependent characteristics are shown in **Figures 1** and **2**, respectively. The resonant and anti-resonant frequencies were measured at 41.38

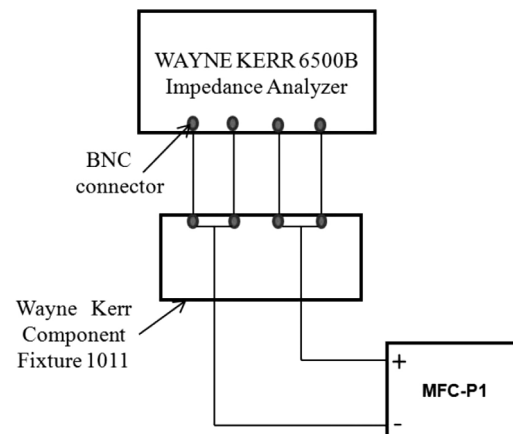


Figure 1: Experimental schematic diagram for impedance and phase measurements of the Macro Fiber Composite transducer (MFC-P1-2814) using the impedance analyzer (Wayne Kerr 6500B)

kHz and 43.63 kHz, respectively. The measured phase jump frequency of 42.58 kHz is also close to these frequencies and therefore, the excitation frequency was chosen as 42 kHz for the subsequent analysis.

In order to analyze the spatial displacements and performance of the d33 (elongation) mode, the 3D displacements (*in-plane* and *out of plane* components) are measured at various spatial points of the unloaded MFC-P1-2814 using the Polytec PSV-500-3D-HV scanning laser vibrometer. A schematic of the experimental set-up is shown in **Figure 3**. The PSV-500-3D-HV laser vibrometer consists of three laser sensor heads. The scanning head (PSV-I-500) with high precision is called as the top head, which contains the full HD camera (20× zoom) for visualization, alignments and video triangulation and the geometry scan unit (PSV-G-500). There are two scanning heads (PSV-I-520), which do not contain the video camera and geometry scan unit and are denoted as left/right scanning heads. The front-end (PSV-F-500-V) unit has three digital broadband decoders and a signal generator. The high-frequency Doppler signal coming from the scanning head is transmitted to the decoder and the velocity information is extracted. The junction box (PSV-E-530) works as an interface between the scanning heads and

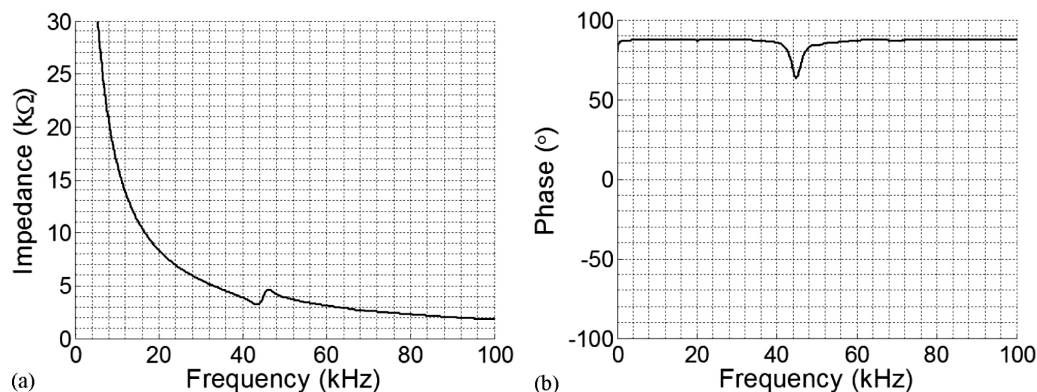


Figure 2: Frequency response of MFC-P1: a) impedance characteristics and b) phase characteristics

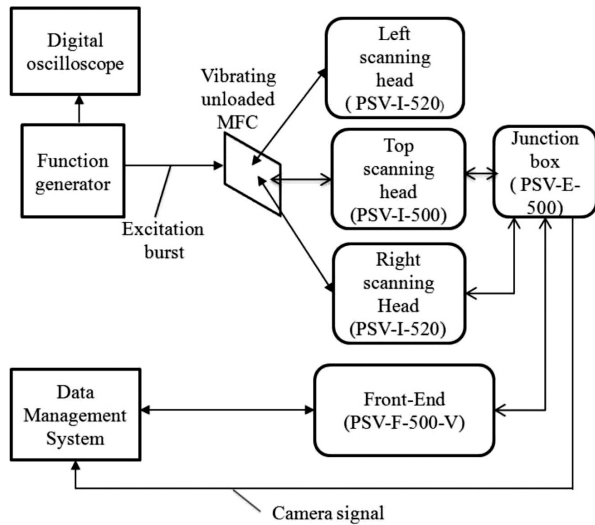


Figure 3: Experimental set-up for 3D displacement measurement using Polytec PSV-500-3D-HV laser vibrometer

the front-end unit. The measurement data is transferred to a PC using an ethernet interface.

The three laser heads must be aligned to each other and to the measurement object (MFC-P1) before conducting the measurements. There are two ways in which positioning of the laser beams on scan points defined on the surface of the vibrating MFC is performed. The first method is the 2D alignment (standard alignment), which is used to position the laser beam, and the scan points can be defined on the live video image. The second method is the 3D alignment in which the angles of spatially scanned mirrors for a given point of the spatial scan are calculated using 3D coordinates. The software itself offers a correction for the measurement coordinates on the live video image and it positions the laser beam to cover all the measurement points using the 3D alignment and finds the spot of the reflected laser beam. Finally, this position will be used instead of the position calculated using the 2D alignment. The achieved accuracy of the laser positions for the top, left and right laser in the experiment was reported as 0.1 mm, 0.2 mm and 0.2 mm, respectively.

Since the active size of the MFC is 28 mm × 14 mm, 17 scanning points are selected along the length with a separation distance of 1.75 mm and the same number of points are selected along the width with a separation distance of 0.875 mm by the data-analysis software of the 3D vibrometer (Polytec). Hence, the total number of scanned points was 289. The MFC is excited by applying a burst-type sinusoidal signal of 120 cycles, a peak-to-peak amplitude of 10V and an operating frequency of 42 kHz. The sampling frequency was 1.25 MHz with a sampling interval of 0.8 μs. Although the 3D displacements are measured at all points, the symmetry of MFC structure means it is only possible to consider the points along the edges (17 points along the length and 17 points along the width). The defined directions of *in-plane* components (*X* and *Y*-components) and *out-of-plane*

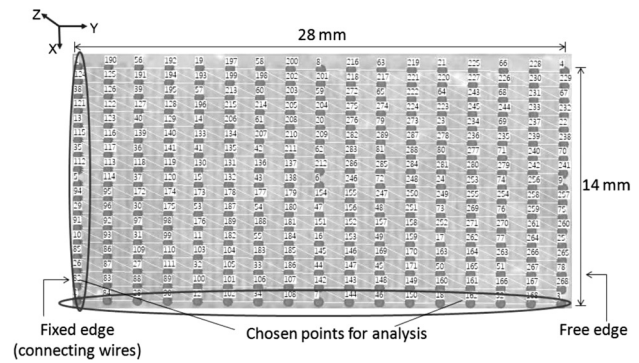


Figure 4: The measured points of interest along the defined directions of the *X*, *Y* and *Z*-displacement components using PSV-500 3D laser vibrometer

component (*Z*-component) of displacements along the chosen points of interest are shown in **Figure 4**. Later, the positive and negative values of the 3D displacements along the length and width of the vibrating unloaded MFC transducer were estimated in order to plot the displacement characteristics.

3 RESULTS AND DISCUSSION

To obtain the correct results, the experiment is performed three times. In each case the variation of peak values from the mean value was observed as less than 1 %. The positive and negative values of the spatial displacements measured along the length (*L*) and width (*W*) of MFC-P1 type transducer are presented in **Figure 5**. It can be easily observed that a change in the amplitudes of the *Y*-displacement component is much higher along the length of MFC, while the *X*-displacement component is higher along the width.

It has also been observed from **Figure 5a** to **5d** that the range of the *Y* displacement is much higher (-167 nm to +167 nm) compared to the *X* displacement (-35 nm to +35 nm) and the *Z*-displacement (-100 nm to +100 nm). This leads to the confirmation that the longitudinal displacement of the MFC-P1 is much higher and it operates in elongation or *d33* mode. This unique feature is quite useful for testing composite materials by mounting on the surface or embedding the MFC or MFC arrays into the structure of the object. The *Z*-displacement (corresponds to the dominant component of the *A0* mode) has the same displacement profile as the *Y*-displacement (corresponds to the dominant component of the *S0* mode) but has a lower amplitude of displacements as described in **Figure 5e** and **Figure 5f**.

There are two types of fundamental Lamb wave modes (the *S0* and *A0*) that can be generated at low frequencies.⁸ The average displacement of the *S0* (symmetric mode) and *A0* (anti-symmetric mode) over the thickness of plate exists in the longitudinal (in the direction of wave propagation) and transverse (out-of-plane) directions, respectively.¹³ Therefore, in-plane *Y* displace-

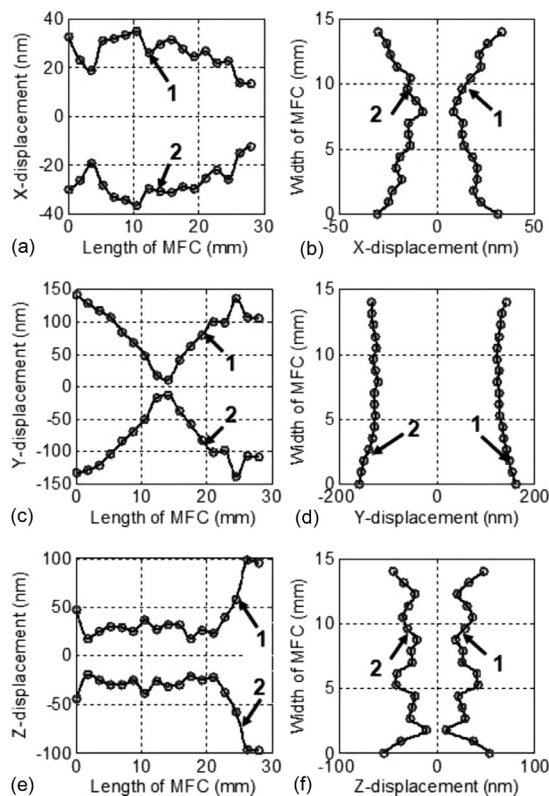


Figure 5: Positive and negative 3D (X, Y and Z) displacements along the length and width, measured at edges of MFC-P1: a) X displacements along the length and b) along the width, c) Y displacements along the length and d) along the width, e) Z displacements along the length and f) along the width (1- measured positive displacements, 2- measured negative displacements)

ments as shown in **Figures 5c, 5d** indicate the performance to generate and receive the S0 mode. The out-of-plane Z displacements as shown in **Figures 5e, 5f** indicate performance to generate and receive the A0 mode. Apart from the fundamental Lamb wave modes (the A0 and S0), the fundamental shear horizontal mode (SH0) is another kind of guided wave that is completely non-dispersive and does not possess the out-of-plane displacements.^{3,14}

As the particle motion of the SH0 mode is *in-plane*, it propagates in the perpendicular direction to the direction of the S0 mode propagation. However, the performance to generate the shear displacements of the SH0 mode should be estimated by both the X and Y displacements (**Figures 5a to 5d**), respectively. It should also be noted that the system of the laser vibrometer is very sensitive to errors and the presence of noise due to a misalignment of the scanning heads, therefore the averaging of 64 was applied and the ambient temperature of 23 °C was maintained throughout the measurement process.

In the next step, interesting results were observed by comparing the displacements at the center of MFC and at the corner point on the longitudinal axis. These two points are shown in **Figure 6** as scanned point No. 6 and scanned point No. 9, respectively. The envelope of the 3D displacements at these points was obtained by

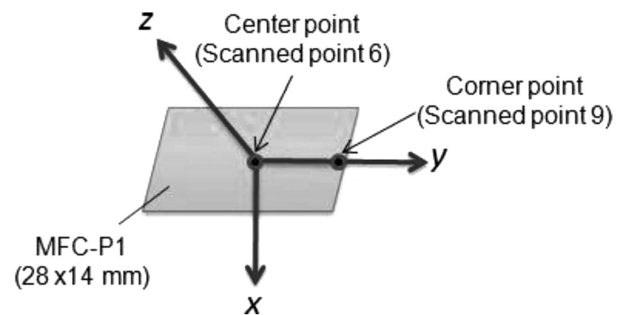


Figure 6: Showing the center point (scanned point 6) and corner point (scanned point 9) on the longitudinal axis of MFC-P1

applying the Hilbert transform (HT) on each of the signals¹⁵. The results are shown in **Figures 7a to 7f**). The time interval is chosen in order to pick up the maximum displacements. After analysing the results, the outcomes can be described as follows.

There is not much difference observed between the maximum X-displacements (10 nm–12.2 nm) in both cases as shown in **Figure 7a** and **Figure 7d**. Moreover, the X-displacement is the minimum among all three displacements. Therefore, the applicability of MFC transducers to generate and pick up the SH0 mode in NDT is not effective.

It can be observed from **Figures 7b** and **7c** that the maximum value of the Z-displacement (*out-of-plane*) is slightly higher than the Y-displacement (along with the

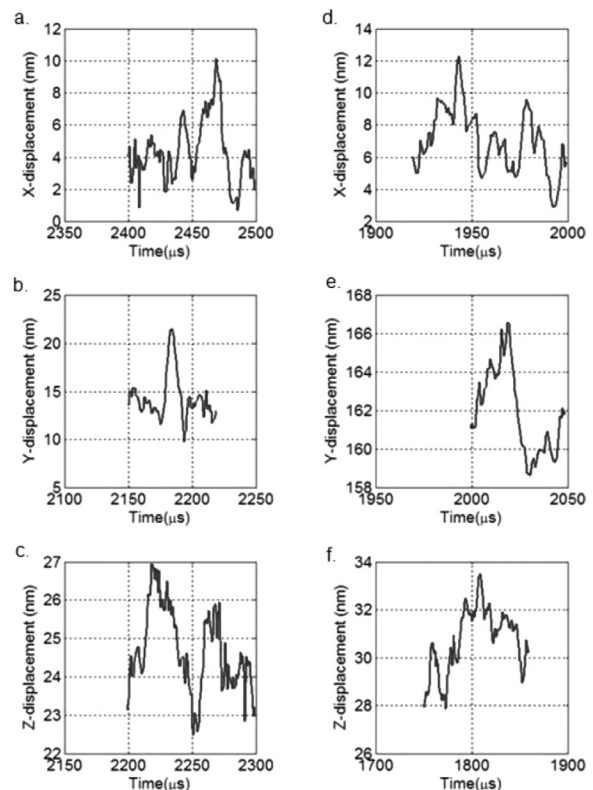


Figure 7: 3D displacements at center (scanning point-6): a), b), c) and corner point (scanned point-9) d), e), f) on the longitudinal axis of MFC-P1

direction of propagation) at the center of MFC. The difference between maximum Z and Y-displacements, in this case, was observed as less than 6 nm.

The rapid increment in the maximum value of the Y-displacement was observed at the corner point (166.7 nm) as compared to the center point (21.5 nm) as shown in **Figure 7b** and **Figure 7e**. On another hand, the X- and Z-displacements were observed as 12.3 nm and 33.5 nm, respectively, at the corner point, as shown in **Figure 7d** and **Figure 7f**, respectively. The rapid change in the maximum Y-displacements from the center to the corner of MFC reconfirms its ability for the effective generation/reception of the S0 mode.

4 CONCLUSIONS

In this paper a macro fiber composite transducer MFC-P1-2814 (Sr. No 08J100791) has been analyzed to estimate its feasibility to be used for NDT and SHM tasks. The impedance and phase characteristics of MFC have been measured using the impedance analyzer (Wayne Kerr 6500B) in order to estimate the resonant and anti-resonant frequency values. Later, values of 3D spatial displacements of the unloaded MFC-P1 operating in the d33 (elongation) mode were measured using a PSV-500-3D-HV (Polytec) scanning laser vibrometer. It should be noted that the measurements were performed three times and high-accuracy results were achieved with less than 1 % variance from the mean value. It was confirmed that the amplitude of *in-plane* longitudinal displacement (Y-component) is the highest among the other X and Z-components. The measured maximum value of the Y displacements is 167 nm. The displacement characteristics at the center point and at the corner of MFC its longitudinal axis were also compared. The maximum X and Z-displacements in both cases did not show a significant difference. On another hand, the maximum Y-displacement showed a significant increment from its value 21.5 nm at the center to 166.7 nm at the corner point that in turn again confirms its operation in elongation mode.

It was also noticed that two different sets of measurements produce the same behaviour that also confirms the existence of systematic errors rather than stochastic ones. The overall displacement characteristics of MFC-P1 confirm that MFC-P1 utilizes the d33 effect and effectively operates in the elongation mode, as described by the manufacturer.¹ Therefore, investigating the 3D displacement characteristics of the transducers in the generation of GW modes is an efficient technique in order to verify the behaviour of the transducer for its conformity in the application of low-frequency ultrasonic NDT and SHM. The transducer, whose 3-dimensional characteristics are not similar to its behaviour, must be omitted and should not be used for further analysis. Moreover,

the 3D displacement profile can positively contribute to the development of analytical and numerical models to predict the directivity patterns of a transducer.

5 REFERENCES

- ¹ MFC. <http://www.smart-material.com/MFC-product-main.html>, 22. 3. 2017
- ² T. Stepinski, M. Mańka, A. Martowicz, Interdigital lamb wave transducers for applications in structural health monitoring, *NDT & E International*. 86 (2017), 199–210, doi:10.1016/j.ndteint.2016.10.007
- ³ A. G. Haig, R. M. Sanderson, P. J. Mudge, W. Balachandran, Macro-fibre composite actuators for the transduction of Lamb and horizontal shear ultrasonic guided waves, *Insight – Non-Destructive Testing and Condition Monitoring*. 55 (2013), 72–77, doi:10.1784/insi.2012.55.2.72
- ⁴ P. Rizzo, H. Matt, S. Coccia, F. L. Di Scalea, I. Bartoli, A. Marzani, E. Viola, Guided ultrasonic waves for the inspection of structural components, *Proceedings of the 16th Italian Conference on Computational Mechanics*, Ubertini, Viola, De Miranda, Castellazzi, eds., Bologna, Italy, 2006
- ⁵ W. K. Wilkie, R. G. Bryant, J. W. High, R. L. Fox, R. F. Hellbaum, J. A. Jalink, B. D. Little, P. H. Mirick, Low cost piezocomposite actuator for structural control applications, *Smart Structures and Materials 2000: Industrial and Commercial Applications of Smart Structures Technologies*, 3991 (2000), 323, doi:10.1117/12.388175
- ⁶ G. Ren, K. Y. Jhang, Application of Macrofiber Composite for Smart Transducer of Lamb Wave Inspection. *Advances in Materials Science and Engineering*, 281575 (2013), 1–5, doi:10.1155/2013/281575
- ⁷ K. A. Tiwari, R. Raisutis, Comparative analysis of non-Contact ultrasonic methods for defect estimation of composites in remote areas, *CBU International Conference Proceedings*, 4 (2016), 846–851, doi:10.12955/cbup.v4.863
- ⁸ R. Pullin, M. J. Eaton, M. R. Pearson, C. Featherston, J. Lees, J. Naylor, A. Kural, D. J. Simpson, K. Holford, On the development of a damage detection system using macro-fibre Composite sensors, *Journal of Physics: Conference Series*, 012049 (2012), 382, doi:10.1088/1742-6596/382/1/012049
- ⁹ W. Xiaoming, Z. Wenya, W.U. Zhigang, Dynamic shape control of wing using piezoelectric fiber composite materials, *Acta Aeronautica et Astronautica Sinica*. 38 (2017), 1–13, doi:10.7527/S1000-6893.2016.0207
- ¹⁰ M. Debiasi, C. W. Leong, Y. Bouremel, C. Y. Yap, Application of macro-fiber-composite materials on UAV wings, *Proceedings of the Aerospace Technology Seminar (ATS)*, Singapore, 2013
- ¹¹ C.B. Scruby, L. E. Drain, *Laser ultrasonics techniques and applications*, CRC Press, 182, 1990
- ¹² K. A. Tiwari, R. Raisutis, L. Mazeika, V. Samaitis, Development of a 2D analytical model for the prediction of directivity pattern of transducers in the generation of guided wave modes, *Procedia Structural Integrity*, 5 (2017), 973–980, doi:10.1016/j.prostr.2017.07.139
- ¹³ K. Worden, Rayleigh and Lamb Waves - Basic Principles, *Strain*, 37 (2001), 167–172, doi:10.1111/j.1475-1305.2001.tb01254.x
- ¹⁴ M. C. Manka, M. Rosiek, A. Martowicz, T. Stepinski, T. Uhl, Lamb wave transducers made of piezoelectric macro-fiber composite. *Structural Control and Health Monitoring*, 20 (2012), 1138–1158, doi:10.1002/stc.1523
- ¹⁵ M. F. Caetano, X. Rodet, Improved estimation of the amplitude envelope of time domain signals using true envelope cepstral smoothing, *IEEE International Conference on Acoustics, Speech and Signal Processing*, Czech Republic, (2011), 11–21, doi:10.1109/icassp.2011.5947290